



SUBGRADIENT ALGORITHM FOR COMPUTING CONTRACTION METRICS FOR EQUILIBRIA

PETER GIESL^{✉1}, SIGURDUR HAFSTEIN^{✉*2}, MAGNEA HARALDSDOTTIR^{✉2},
DAVID THORSTEINSSON^{✉2} AND CHRISTOPH KAWAN^{✉3}

¹Department of Mathematics
University of Sussex
Falmer, BN1 9QH, UK

²The Science Institute, University of Iceland
Dunhagi 5
107 Reykjavik, Iceland

³Institute of Informatics, LMU Munich
Oettingenstraße 67
80538 Munich, Germany

(Communicated by Oliver Junge)

ABSTRACT. We propose a subgradient algorithm for the computation of contraction metrics for systems with an exponentially stable equilibrium. We show that for sufficiently smooth systems our method is always able to compute a contraction metric on any forward-invariant compact neighbourhood of the equilibrium, which is a subset its basin of attraction. We demonstrate the applicability of our method by constructing contraction metrics for three planar and one three-dimensional systems.

Contraction metrics; stability analysis; contraction metrics; subgradient method

1. Introduction. Consider an ordinary differential equation (ODE)

$$\dot{x} = f(x) \tag{1.1}$$

with a C^1 -vector field $f : \mathbb{R}^n \rightarrow \mathbb{R}^n$; we will denote the Jacobian of f by $Df(x)$. Let $\phi^t(x)$ denote the induced flow, i.e. the solution of (1.1) at time $t \geq 0$ with initial value x , and assume that it is defined for all $t \geq 0$. Furthermore, we assume that $K \subset \mathbb{R}^n$ is a compact forward-invariant set which is the closure of its interior, i.e. $\overline{K^\circ} = K$.

An *equilibrium* of the ODE is a point $x_0 \in \mathbb{R}^n$ such that $f(x_0) = 0$, from which $\phi^t(x_0) = x_0$ for all $t \geq 0$ follows. The equilibrium is said to be *exponentially stable* if there exist $\delta, \rho, C > 0$ such that $\|x - x_0\| < \delta$ implies

$$\|\phi^t(x) - x_0\| \leq C\|x - x_0\|e^{-\rho t} \quad \text{for all } t \geq 0,$$

2020 *Mathematics Subject Classification.* Primary: 37C75, 93D05, 37M22; Secondary: 39A30, 34D20.

Key words and phrases. Contraction metric, differential equation, exponentially stable equilibrium.

The second author is supported in part by the Icelandic Research Fund under Grant 228725-051.

*Corresponding author: Sigurdur Hafstein.

where $\rho > 0$ is called the *rate of exponential attraction*; here and elsewhere in the paper, $\|\cdot\|$ stands for the Euclidean norm on \mathbb{R}^n . We denote by $A(x_0) = \{x \in \mathbb{R}^n : \lim_{t \rightarrow \infty} \phi^t(x) = x_0\}$ its *basin of attraction*.

It is usually not hard to compute the equilibria by solving $f(x) = 0$. Further, the exponential stability of an equilibrium x_0 can be determined from the eigenvalues of the linearization $Df(x_0)$ of f at x_0 ; the equilibrium is exponentially stable if and only if the real part of each eigenvalue of $Df(x_0)$ is strictly negative. Estimating $A(x_0)$ is a much harder problem.

We are interested in proving the existence, uniqueness and exponential stability of an equilibrium x_0 , as well as gaining information on its basin of attraction. There are different methods in the literature towards estimating the basin of attraction. A lower bound can be obtained by computing a Lyapunov function for the system [29, 34]. Computing a Lyapunov function analytically is usually not feasible for a nonlinear system, therefore a plethora of numerical methods have been developed. To name a few, a sum of squared (SOS) polynomials Lyapunov function can be parametrized by using semidefinite programming [36], an approximate solution to the Zubov equation [44] can be obtained by collocation with radial basis functions (RBF) [14], or linear programming can be used to parametrize a continuous and piecewise affine (CPA) Lyapunov function [22, 26]. For an overview of numerical methods to construct Lyapunov functions, see, e.g., the review [17].

Other methods to compute the basin of attraction of an equilibrium include determining its boundary by computing invariant manifolds [31], or dividing the phase space into cells using the cell mapping approach [24] or set oriented methods [10] and computing the dynamics between those cells [35].

Another approach for studying the basin of attraction is based on contraction metrics, which has the advantage that the position of the equilibrium is not needed. While a Lyapunov function shows that solutions approach the equilibrium as time evolves, a contraction metric proves that adjacent solutions approach each other as time evolves when measured by an appropriate Riemannian metric [1, 23, 30, 33].

Converse theorems, proving the existence of a contraction metric, have been derived in [15]. The explicit analytical computation of a contraction metric is, however, in most cases not achievable. Numerical methods to compute contraction metrics are often similar to the ones used to compute Lyapunov functions, e.g. in [6, 7] metrics with SOS polynomial entries are computed, in [21] collocation with RBF is used, in [16] a CPA contraction metric is parametrized using semidefinite programming, and in [19] collocation with RBF is used to obtain an approximation that is subsequently verified by CPA. See the recent review [18] for an overview of methods for the computation of contraction metrics.

Let us compare the various methods with the proposed method in this paper: the SOS method computes a polynomial matrix-valued contraction metric. Since not all positive definite functions are sums of squares, there is no guarantee that an SOS contraction metric exists. The algorithm transforms the conditions of a contraction metric into Linear Matrix Inequalities. For the algorithm, a maximal degree of the polynomials needs to be fixed in advance, which might not be sufficiently high. An SOS contraction metric is valid for the entire \mathbb{R}^n and thus shows global stability, moreover it rigorously proves the properties of a contraction metric.

For the CPA method, a triangulation of a compact subset of the phase space is fixed, and the contraction metric is found as a continuous piecewise affine function on each simplex of the triangulation. The conditions are transformed into

constraints of a semi-definite programming problem. If a contraction metric exists and the triangulation is sufficiently fine, the method is guaranteed to find a CPA contraction metric, however the method only works on compact subsets. Due to inbuilt Taylor-type error estimates, the method rigorously proves the properties of a contraction metric.

The collocation method constructs a contraction metric as the approximation of a solution of a certain matrix-valued PDE after fixing a finite number of collocation points, which may be scattered. Practically, the solution is found by solving a system of linear equations. If a contraction metric exists and the collocation points are sufficiently dense, the method is guaranteed to find a contraction metric. However the method only works on compact subsets and an a posteriori error estimate is necessary to rigorously prove the properties of a contraction metric.

In this paper, we adapt the subgradient method from [28], developed for obtaining upper bounds on the restoration entropy for dynamical systems, to compute a contraction metric for an equilibrium of (1.1) on a compact set $K \subset \mathbb{R}^n$. For some recent references on the subgradient method and its variations see, e.g. [2, 43, 42, 3, 4, 5].

In comparison to the other methods, we also consider a compact subset, similar to all methods apart from the SOS method. Our method is based on iterations and thus can be pursued until a contraction metric is found. A contraction metric of the form $e^{p(x)}P$ with a constant matrix P and polynomial of maximal fixed degree is constructed. While the properties of a contraction metric are asserted on a dense set, an a posteriori error estimate would be necessary to rigorously prove the properties of a contraction metric, similar to the RBF method. Similarly to the SOS method, the algorithm finds a bound for the exponential attraction. Finally, the method is fast and can compute 10,000 iterations in minutes to hours, depending on the degree of the polynomial and number of points used in the minimization in the method.

The paper is structured as follows: in Section 2 some basic definitions and results about Riemannian contraction metrics are provided, in particular we recall results that describe their implications and guarantee their existence for systems with an exponentially stable equilibrium.

Section 3 contains the main theoretical contributions of the paper: first we develop our method to compute contraction metrics for system (1.1) on compact sets $K \subset \mathbb{R}^n$. Then we prove a new converse theorem for system (1.1), assuming it admits an exponentially stable equilibrium and that $f \in C^{n+2}$; see the precise requirements in the theorem. Theorem 3.1 assures the existence of a contraction metric of the specific form $M(x) = e^{p(x)}P$, $P \in \mathbb{R}^{n \times n}$ symmetric and positive definite and $p: \mathbb{R}^n \rightarrow \mathbb{R}$ a polynomial. In Section 4, we adapt the subgradient method from [28] as needed for our approach. In Section 5, we show the application of our algorithm to four examples, before concluding in Section 6.

Notation. If $A \subset \mathbb{R}^n$, we write \bar{A} and A° for the closure and the interior of A , respectively. For the Euclidean norm of a vector $x \in \mathbb{R}^n$, we write $\|x\|$. We denote by \mathcal{S}_n the set of symmetric $\mathbb{R}^{n \times n}$ matrices and by \mathcal{S}_n^+ the set of symmetric and positive definite $\mathbb{R}^{n \times n}$ matrices. Further, for $A, B \in \mathcal{S}_n$ we write $A \succ B$ or $B \prec A$ if $A - B \in \mathcal{S}_n^+$ and $A \succeq B$ or $B \preceq A$ if $A - B$ is positive semi-definite. We denote the trace of a matrix $A \in \mathbb{R}^{n \times n}$ by $\text{tr}(A)$. For a set $K \subset \mathbb{R}^n$ and $\delta > 0$, we define $K_\delta := \{x \in \mathbb{R}^n : d(x, K) < \delta\}$, where $d(x, K) := \inf_{y \in K} \|x - y\|$.

2. Contraction metrics. In this section, we review basic concepts about Riemannian contraction metrics and some important tools that we will use later in this paper.

Definition 2.1 (Riemannian metric). Let G be an open subset of \mathbb{R}^n . A Riemannian metric on G is a continuously differentiable matrix-valued function $M \in C^1(G, \mathcal{S}_n^+)$.

A Riemannian metric M defines a (point-dependent) scalar product $\langle v, w \rangle_{M(x)} := v^T M(x) w$ for each $x \in G$ and all $v, w \in \mathbb{R}^n$.

The orbital derivative $\dot{M}(x)$ with respect to (1.1) at $x \in G$ is defined by

$$\dot{M}(x) := \left. \frac{d}{dt} M(\phi^t(x)) \right|_{t=0} = \left(\nabla M_{ij}(x) \cdot f(x) \right)_{ij}.$$

The second equality is a consequence of the chain rule and $(a_{ij})_{ij}$ denotes the matrix with entries a_{ij} , $i, j = 1, \dots, n$.

Definition 2.2 (Contraction metric). Let K be a compact subset of an open set $G \subset \mathbb{R}^n$ and $M \in C^1(G, \mathcal{S}_n^+)$ a Riemannian metric. For $x \in K$, $v \in \mathbb{R}^n$, define

$$L_M(x; v) := \frac{1}{2} v^T [M(x) Df(x) + Df(x)^T M(x) + \dot{M}(x)] v.$$

The Riemannian metric is called contracting in $K \subset G$ for system (1.1) with exponent $-\nu < 0$, or a *contraction metric* on K , if

$$\begin{aligned} \mathcal{L}_M(x) &\leq -\nu \text{ for all } x \in K, \text{ where} \\ \mathcal{L}_M(x) &:= \max_{v^T M(x) v = 1} L_M(x; v). \end{aligned} \tag{2.1}$$

Remark 2.3. Fix $x \in K$. Note that (2.1) is equivalent to

$$M(x) Df(x) + Df(x)^T M(x) + \dot{M}(x) \preceq -2\nu M(x), \tag{2.2}$$

see [15, Rem. 2.5].

The existence of a contraction metric for system (1.1) is both a sufficient and a necessary condition for the existence of an exponentially stable equilibrium. We state the former in the next theorem and prove the latter in a specific form for our needs in Theorem 3.1; for a converse theorem with less smoothness requirements on the system, see [15, Thms. 2.2, 2.3]. We cite Theorem 3.1 from [15] in the next theorem.

Theorem 2.4 (Existence and uniqueness of the equilibrium). *Let $\emptyset \neq K \subset \mathbb{R}^n$ be a compact, connected and forward-invariant invariant set and M a Riemannian metric defined on a neighborhood G of K and contracting in K with exponent $-\nu < 0$. Then there exists one and only one equilibrium x_0 of system (1.1) in K ; x_0 is exponentially stable with rate of exponential attraction ν , and K is a subset of its basin of attraction $A(x_0)$.*

3. Converse theorem for contraction metrics. The class $C_d(K)$ of conformal metrics of the form $M(x) = e^{p(x)} P$, $p: \mathbb{R}^n \rightarrow \mathbb{R}$ a polynomial of degree $\leq d$ and $P \in \mathcal{S}_n^+$, was used in [28] because it is geodesically convex, cf. [28, Lem. 4.1], and parametrized by a finite number of parameters. Further, in several examples an analytical expression for a Riemannian metric of this class is known, which gives the exact value for the restoration entropy. However, there certainly are some

limitations by restricting the search for a metric to this class. For our task of computing contraction metrics for exponentially stable equilibria, it is, however, not limiting as shown in Theorem 3.1. Hence, it is particularly well-suited for our algorithm.

In the proof of Theorem 3.1, we use results about the existence of polynomial Lyapunov functions from [37, Thm. 9] for system (1.1).

Theorem 3.1. *Let x_0 be an exponentially stable equilibrium of system (1.1) and assume that $f \in C^{n+2}(\mathbb{R}^n, \mathbb{R}^n)$. Denote by $-\nu$ the largest real part of all eigenvalues of $Df(x_0)$. Furthermore, assume that $K = \overline{K^\circ} \subset A(x_0)$ is compact and forward-invariant. Then there exists a Riemannian contraction metric on K of the form $M(x) = e^{p(x)}P$, where $p: \mathbb{R}^n \rightarrow \mathbb{R}$ is a polynomial and $P \in \mathcal{S}_n^+$. Further, for every $\varepsilon > 0$, there exists M of the form above such that $\mathcal{L}_M(x) \leq -\nu + \varepsilon$ for all $x \in K$.*

Proof. We assume w.l.o.g. that $x_0 = 0$. We first establish the existence of a polynomial Lyapunov function for (1.1): Note that there are constants $\rho > 0$ and $C \geq 1$ such that for all $x \in K$ and $t \geq 0$ the estimate $\|\phi^t(x)\| \leq C\|x\|e^{-\rho t}$ holds true; see e.g. [8, Lem. 1]. By a standard argumentation identical to e.g. the proof of [29, Thm. 4.14] or [40, Ch. 5, Thm. 63], one can then show that for a large enough $T > 0$ the function $V(x) = \int_0^T \|\phi^t(x)\|^2 dt$ is a Lyapunov function fulfilling the inequalities

$$\begin{aligned} \alpha_0\|x\|^2 &\leq V(x) \leq \beta_0\|x\|^2, \\ \dot{V}(x) &\leq -\gamma_0\|x\|^2 \end{aligned} \tag{3.1}$$

for some constants $\alpha_0, \beta_0, \gamma_0 > 0$ and for all $x \in K$. Since $f \in C^{n+2}(\mathbb{R}^n, \mathbb{R}^n)$ so is $(t, x) \mapsto \phi^t(x)$, see e.g. [41, III.§13.XI], and it follows that $V \in C^{n+2}(K, \mathbb{R})$ because we can differentiate under the integral over a compact interval.

We can use standard techniques of smoothing by convolution with a smooth kernel to extend V from K to a function $\tilde{V} \in C^{n+2}(\mathbb{R}^n, \mathbb{R})$ with $\tilde{V}(x) = V(x)$ for $x \in K$ and $\tilde{V}(x) = 1$ for $x \in \mathbb{R}^n \setminus K_{\tilde{\delta}}$, with $\tilde{\delta} > 0$ so small that $K_{\tilde{\delta}} \subset A(0)$. Thus, we may assume that V fulfilling (3.1) is in $C^{n+2}(\mathbb{R}^n, \mathbb{R})$ and apply [37, Thm. 9] to assert for every $\alpha \in (0, \alpha_0)$, $\beta > \beta_0$, and $\gamma \in (0, \gamma_0)$ the existence of a polynomial Lyapunov function $W: \mathbb{R}^n \rightarrow \mathbb{R}$ fulfilling

$$\begin{aligned} \alpha\|x\|^2 &\leq W(x) \leq \beta\|x\|^2, \\ \dot{W}(x) &\leq -\gamma\|x\|^2 \end{aligned} \tag{3.2}$$

for all $x \in K$.

We now complete the proof following the proof of [15, Thm. 4.1]: Fix an $\varepsilon \in (0, \nu)$. As in Step 1 of the proof of [15, Thm. 4.1], one can show there exists a $P \in \mathcal{S}_n^+$ such that $\mathcal{L}_P(0) \leq -\nu + \frac{\varepsilon}{2}$, using a special Jordan Normal Form of $Df(0)$. Set

$$\mu(x) := \mathcal{L}_P(x) = \max_{v^\top P v = 1} \frac{1}{2} v^\top [PDf(x) + Df(x)^\top P] v \tag{3.3}$$

and $\mu^* := \max_{x \in K} \mu(x)$.

If $\mu^* \leq -\nu + \varepsilon < 0$ we can set $p(x) := 0$ and the statements of the theorem hold true with $M(x) := e^{p(x)}P = P$ for all $x \in K$, because $\max_{x \in K} \mathcal{L}_M(x) = \mu^* < 0$.

Now assume that $\mu^* > -\nu + \varepsilon$, set $c := \frac{\mu^* + \nu - \varepsilon}{\gamma \delta^2} > 0$, define the polynomial $p(x) := 2cW(x)$, and set $M(x) := e^{p(x)}P$ for all $x \in K$. The function M is a Riemannian metric and from

$$2\mathcal{L}_M(x; v) = e^{p(x)}v^\top [PDf(x) + Df(x)^\top P + 2c\dot{W}(x)P]v$$

$$= e^{p(x)} v^\top [PDf(x) + Df(x)^\top P] v + e^{p(x)} 2c\dot{W}(x) v^\top P v$$

and (3.3), we see that

$$\mathcal{L}_M(x) = \max_{v^\top M(x)v=1} L_M(x;v) = \max_{v^\top P v=e^{-p(x)}} L_M(x;v) = \mu(x) + c\dot{W}(x).$$

Since μ is a continuous function (see [15, Lem. 2.6]), there is a $\delta > 0$ such that $B_\delta(0) \subset K$ and $x \in B_\delta(0)$ implies $\mu(x) \leq -\nu + \varepsilon$; recall that $\mu(0) = \mathcal{L}_P(0) \leq -\nu + \frac{\varepsilon}{2}$.

We show that $\mu(x) \leq -\nu + \varepsilon$ for all $x \in K$ by distinguishing between two cases:

Case (i). Assume that $x \in B_\delta(0)$. Then, since $\dot{W}(x) \leq 0$, we have

$$\mathcal{L}_M(x) = \mu(x) + c\dot{W}(x) \leq -\nu + \varepsilon.$$

Case(ii). Assume that $x \in K \setminus B_\delta(0)$. Then $\dot{W}(x) \leq -\gamma\delta^2$ by (3.2) and we have, using (3.3),

$$\mathcal{L}_M(x) = \mu(x) + c\dot{W}(x) \leq \mu^* - c\gamma\delta^2 = \mu^* - (\mu^* + \nu - \varepsilon) = -\nu + \varepsilon.$$

This concludes the proof. \square

Remark 3.2. Note that Theorem 3.1 and its proof do not provide the degree of the polynomial p in $M(x) = e^{p(x)}P$. For polynomial right-hand sides f in (1.1), degree bounds that depend on the size of K , $\max_{x \in K} \|\nabla f(x)\|$, and the parameters ρ in C in the estimate $\|\phi(t, x)\| \leq C\|x\|e^{-\rho t}$ are available, see [38]. However, these bounds are somewhat conservative and not applicable to non-polynomial f .

Remark 3.3. In [37] less strict assumptions on the smoothness of f in Theorem 3.1 are used. However, we use the assumption $f \in C^{n+2}(\mathbb{R}^n, \mathbb{R}^n)$, from which $(t, x) \mapsto \phi^t(x)$ in C^{n+2} definitely follows, see e.g. [41, III.§13.XI]. In the arXiv version of the paper [37] this is also the assumption used.

4. Subgradient algorithm for contraction metrics. We now adapt the subgradient algorithm from [28], which was used for the approximation of the restoration entropy, to compute contraction metrics for system (1.1). The main idea is the following: Assume that $M \in C^1(G, \mathcal{S}_n^+)$ is a Riemannian metric on the open set $G \supset K$, K compact. Fix $x \in K$, and let λ_i , $i = 1, \dots, n$, be the solutions to (roots of the polynomial)

$$\det[Df(x)^\top M(x) + M(x)Df(x) + \dot{M}(x) - \lambda M(x)] = 0. \quad (4.1)$$

Then the λ_i are the eigenvalues of the symmetric matrix

$$A(x) := M^{-\frac{1}{2}}(x)[M(x)Df(x) + Df(x)^\top M(x) + \dot{M}(x)]M^{-\frac{1}{2}}(x),$$

i.e. $\lambda_i \in \mathbb{R}$ for $i = 1, \dots, n$, and there exists a basis for \mathbb{R}^n of corresponding orthonormal eigenvectors v_i of $A(x)$. By writing an arbitrary $v \in \mathbb{R}^n$ as a linear combination $\sum_{i=1}^n c_i v_i$, $c_i \in \mathbb{R}$, we see that

$$v^\top A(x)v = \left(\sum_{i=1}^n c_i v_i\right)^\top A(x) \sum_{i=1}^n c_i v_i = \sum_{i=1}^n \lambda_i c_i^2$$

and defining $\lambda_{\max} := \max_{i=1, \dots, n} \lambda_i$ delivers

$$v^\top A(x)v \leq \max_{i=1, \dots, n} \lambda_i \|v\|^2 = \lambda_{\max} \|v\|^2.$$

Hence $A(x) \preceq \lambda_{\max} I$, or equivalently $v^\top (A(x) - \lambda_{\max} I)v \leq 0$ for all $v \in \mathbb{R}^n$. With $w = M^{-\frac{1}{2}}(x)v$, we obtain

$$w^\top [M^{\frac{1}{2}}(x)A(x)M^{\frac{1}{2}}(x) - \lambda_{\max} M(x)]w \leq 0 \quad \text{for all } w \in \mathbb{R}^n,$$

which translates into

$$M(x)Df(x) + Df(x)^\top M(x) + \dot{M}(x) \preceq \lambda_{\max} M(x).$$

Hence, we have shown the following proposition by the arguments above and Remark 2.3.

Proposition 4.1. *Let $M \in C^1(G, \mathcal{S}_n^+)$, where $G \subset \mathbb{R}^n$ is open and $K \subset G$ is compact. Denote by $\zeta_1^M(x) \geq \zeta_2^M(x) \geq \dots \geq \zeta_n^M(x)$ the solutions $\zeta(x)$ of*

$$\det[M(x)Df(x) + Df(x)^\top M(x) + \dot{M}(x) - \zeta(x)M(x)] = 0. \quad (4.2)$$

Assume that $\zeta_1^M(x) \leq -2\nu$ holds for all $x \in K$. Then

$$M(x)Df(x) + Df(x)^\top M(x) + \dot{M}(x) \preceq -2\nu M(x),$$

i.e. the Riemannian metric M is contracting on K with exponent ν if $\nu > 0$.

We are thus interested in finding

$$-\nu := \frac{1}{2} \inf_{M \in C^1(G, \mathcal{S}_n^+)} \max_{x \in K} \zeta_1^M(x). \quad (4.3)$$

If $-\nu < 0$, then ν is the rate of exponential attraction of the equilibrium and, moreover, a minimizer M is a corresponding contraction metric.

4.1. The subgradient algorithm on Riemannian manifolds. In this subsection, we briefly explain the subgradient algorithm on a complete Riemannian manifold \mathcal{M} with lower bounded sectional curvature. In particular, we write $T_x \mathcal{M}$ for the tangent space to \mathcal{M} at x and $\langle \cdot, \cdot \rangle_x$ for the inner product on $T_x \mathcal{M}$ given by the Riemannian metric. A function $g : \mathcal{M} \rightarrow \mathbb{R}$ is called geodesically convex if the composition $g \circ \gamma : [0, 1] \rightarrow \mathbb{R}$ is a convex function in the usual sense for every geodesic $\gamma : [0, 1] \rightarrow \mathcal{M}$.

Recall the following facts for a geodesically convex function $g : \mathcal{M} \rightarrow \mathbb{R}$ defined on a complete Riemannian manifold \mathcal{M} [39]:

- g is locally Lipschitz continuous [39, Cor. 3.10].
- Given $x \in \mathcal{M}$, a vector $s \in T_x \mathcal{M}$ is called a *subgradient* of g at x if for any geodesic γ of \mathcal{M} with $\gamma(0) = x$ the following inequality holds:

$$(g \circ \gamma)(\theta) \geq g(x) + \theta \langle s, \dot{\gamma}(0) \rangle_x \quad \text{for all } \theta \geq 0.$$

The set of all subgradients of g at x , denoted by $\partial g(x)$, is called the *subdifferential* of g at x . The subdifferential at any point x is nonempty, convex and compact [39, Thm. 4.5 and 4.6].

The *subgradient algorithm* consists of the following steps for a given sequence $(t_j)_{j \in \mathbb{N}}$ of step sizes with $t_j > 0$ for all j (see also (4.4)):

- (0) Initialize. Choose $p_1 \in \mathcal{M}$ and compute some $s_1 \in \partial g(p_1)$. Put $j := 1$.
- (1) If $s_j = 0$ go to (4). Otherwise, compute the geodesic γ_{v_j} with $\gamma_{v_j}(0) = p_j$, $\dot{\gamma}_{v_j}(0) = v_j$, $v_j = -s_j/|s_j|$, where $|s_j| = \sqrt{\langle s_j, s_j \rangle_{p_j}}$.
- (2) Put $p_{j+1} := \gamma_{v_j}(t_j)$.
- (3) Compute some $s_{j+1} \in \partial g(p_{j+1})$. Put $j := j + 1$ and go to (1).
- (4) p_j is the minimum of g .

The computation of the subgradients and the geodesics is discussed in detail in the next section. For the convergence of the sequence p_j to a minimizer, a proper choice of the step sizes t_j is necessary, and it is an important assumption that the sectional curvature of \mathcal{M} is uniformly bounded from below. The *diminishing or exogeneous step size rule* requires to choose the step sizes t_j such that

$$\sum_{j=1}^{\infty} t_j = \infty \quad \text{and} \quad \sum_{j=1}^{\infty} t_j^2 < \infty. \quad (4.4)$$

Assuming that the sectional curvature of M is uniformly bounded below, with such a choice (typically, $t_j = a/(j+b)$ with $a > 0$, $b \geq 0$), [12, Thm. 3.2] guarantees that

$$\liminf_{j \rightarrow \infty} g(p_j) = \inf_{x \in K} g(x)$$

and that p_j converges to a minimizer, if a minimizer exists.

4.2. The algorithm. To apply the algorithm described in the preceding subsection to solve the problem posed by (4.3), we restrict ourselves to Riemannian metrics of the form

$$M(x) = e^{p_a(x)} P,$$

where $P \in \mathcal{S}_n^+$, $p_a(x) = \sum_{\alpha \in J} a_\alpha x^\alpha$ is a polynomial, and $J \subset \mathbb{N}_0^n$ a finite set of multi-indices. Note that the metric M is parameterized by the matrix P and the vector $a = (a_\alpha)_{\alpha \in J} \in \mathbb{R}^{|J|}$. We have shown in Theorem 3.1 that this class is sufficient to find a contraction metric.

Hence, we restrict the search for the optimal metric to the space $\mathbb{R}^{|J|} \times \mathcal{S}_n^+$, where $\mathbb{R}^{|J|}$ is equipped with the usual Euclidean metric and \mathcal{S}_n^+ with its standard Riemannian metric given by

$$\langle V, W \rangle_P := \text{tr}(P^{-1}VP^{-1}W) \quad \text{for all } P \in \mathcal{S}_n^+, V, W \in T_P\mathcal{S}_n^+ = \mathcal{S}_n.$$

The optimization is performed using the Riemannian subgradient algorithm for geodesically convex functions on the Riemannian product manifold $\mathcal{M} := \mathbb{R}^{|J|} \times \mathcal{S}_n^+$, cf. [13, 12]. The required geodesic convexity of the objective function

$$g: (a, P) \mapsto \max_{x \in K} \zeta_1^{e^{p_a(\cdot)} P}(x) \quad (4.5)$$

is shown in the proof of [28, Lem. 3.5]: in particular,

$$(a, P) \mapsto \max_{x \in K} \sum_{i=1}^k \zeta_i^{e^{p_a(\cdot)} P}(x)$$

is geodesically convex for any $k \in \{1, \dots, n\}$, see inequality (3.6) and equation (3.7) in [28]. The sectional curvature of \mathcal{M} is bounded below by [28, Lem. A.1]. The existence of near-minimizers is guaranteed by Theorem 3.1.

Our algorithm to compute a contraction metric for system (1.1) can be stated as follows:

- (0) Fix some initial values for a and P , e.g. $a_0 = 0$ and $P_0 = I$, and a sequence of step sizes t_j satisfying

$$\sum_{j=1}^{\infty} t_j = \infty \quad \text{and} \quad \sum_{j=1}^{\infty} t_j^2 < \infty.$$

- (1) Step $j = 1, \dots$: Find an $x^* \in K$ that maximizes $g(x; a_j, P_j) = \zeta_1^M(x)$ with $M(x) = e^{p_a(x)} P$.

- (2) Compute a subgradient $s_j \in \partial g(x^*; a_j, P_j)$, where $g(x^*; a_j, P_j) = g(a_j, P_j)$.
- (3) Normalize s_j to unit length by defining $\bar{s}_j := s_j/|s_j|$. Here, $|\cdot|$ is the norm on the product tangent space $T_{(a_j, P_j)}(\mathbb{R}^{|J|} \times \mathcal{S}_n^+) = \mathbb{R}^{|J|} \times \mathcal{S}_n$, given by

$$|s_j| = |(s_j^1, s_j^2)| = \sqrt{\|s_j^1\|^2 + \text{tr}(P_j^{-1} s_j^2 P_j^{-1} s_j^2)},$$

where $\|s_j^1\|$ is the standard Euclidean metric of s_j^1 .

- (4) Update the Riemannian metric by

$$(a_{j+1}, P_{j+1}) := (a_j - t_j \bar{s}_j^1, \exp_{P_j}(-t_j \bar{s}_j^2)).$$

- (5) Let $j \rightarrow j+1$ and go to (1).

Here, $\exp_{P_j}(\cdot)$ is the Riemannian exponential map of \mathcal{S}_n^+ at $P_j \in \mathcal{S}_n^+$, and $\bar{s}_j^1 \in \mathbb{R}^{|J|}$, $\bar{s}_j^2 \in T_{P_j} \mathcal{S}_n^+ = \mathcal{S}_n$ are the two components of \bar{s} . An explicit formula is

$$\exp_{P_j}(-t_j \bar{s}_j^2) = P_j^{1/2} \exp(-t_j P_j^{-1/2} \bar{s}_j^2 P_j^{-1/2}) P_j^{1/2},$$

where \exp on the right-hand side is the usual matrix exponential map.

The details of the computation of the subgradient are given in [28, Sec. 5.2]. Here, we recall the necessary computational steps. For better readability, we omit the index j related to the step of the algorithm and write $B(x) = \text{D}f(x)$ for all $x \in K$. We can then decompose

$$\zeta_1^{\text{e}^{Pa(\cdot)} P}(x) = \dot{p}_a(x) + \lambda_1 (P^{\frac{1}{2}} B(x) P^{-\frac{1}{2}} + P^{-\frac{1}{2}} B(x)^\top P^{\frac{1}{2}})$$

and compute the components s^1 and s^2 of the subgradient $s = (s^1, s^2)$ separately. That is, we compute the subgradient s^1 of $a \mapsto \dot{p}_a(x^*)$ and the subgradient s^2 of $P \mapsto \lambda_1 (P^{\frac{1}{2}} B(x^*) P^{-\frac{1}{2}} + P^{-\frac{1}{2}} B(x^*)^\top P^{\frac{1}{2}})$ and then set $s = (s^1, s^2)$. The component s^1 is trivial, because $\dot{p}_a(x)$ is a linear function of a . The computation of the second component s^2 can be accomplished by processing the following steps:

- Compute an orthonormal basis $\{e_i\}$ of the tangent space $T_P \mathcal{S}_n^+ = \mathcal{S}_n$ with respect to its inner product $\langle \cdot, \cdot \rangle_P$.
- Diagonalize the symmetric matrix

$$X := P^{\frac{1}{2}} B(x^*) P^{-\frac{1}{2}} + P^{-\frac{1}{2}} B(x^*)^\top P^{\frac{1}{2}},$$

leading to $X = U D U^\top$ with $D = \text{diag}(\lambda_1, \dots, \lambda_n)$ and $\lambda_1 \geq \dots \geq \lambda_n$.

- Compute $S := U \text{diag}(1, 0, \dots, 0) U^\top$.
- For each basis vector $e_i \in \mathcal{S}_n$, compute the unique solution Y_i of the Lyapunov equation

$$P^{\frac{1}{2}} Y_i + Y_i P^{\frac{1}{2}} = e_i.$$

- For each Y_i , compute the matrix

$$\begin{aligned} Z_i := & Y_i B(x^*) P^{-\frac{1}{2}} - P^{\frac{1}{2}} B(x^*) P^{-\frac{1}{2}} Y_i P^{-\frac{1}{2}} \\ & - P^{-\frac{1}{2}} Y_i P^{-\frac{1}{2}} B(x^*)^\top P^{\frac{1}{2}} + P^{-\frac{1}{2}} B(x^*)^\top Y_i. \end{aligned}$$

- Compute the subgradient via

$$s^2 = \sum_i \text{tr}[S^\top Z_i] e_i.$$

5. Examples. In this section we demonstrate our algorithm by computing contraction metrics for three planar systems and one three-dimensional system. One of the planar systems has two equilibria and we compute contraction metrics in a neighbourhood of each. In order to obtain a contraction metric one must compute a Riemannian metric on a superset of a forward-invariant set of the dynamics. Thus, one must first locate a forward-invariant set. In Example 5.1 we compute analytically a forward-invariant quadrilateral set, mainly for demonstration. Example 5.2 is taken from [19] and Example 5.4 is taken from [20] and we use the forward-invariant sets computed numerically in these papers. In Example 5.3 we compute a forward invariant set with the method from [19]. In more detail, we approximate the solution of $V'(x) = -\sqrt{10^{-8} + \|f(x)\|^2}$ by a function v and verify that $v'(x) < 0$ holds for all $x \in \partial L_R$, where $L_R = \{x \in \mathbb{R}^n \mid v(x) \leq R\}$ is a sublevel set of v of level $R > 0$. This is rigorously verified using a CPA interpolation and Taylor-like error estimates, and thus shows that L_R is positively invariant.

Example 5.1 is also in [19] and we compute a contraction metric for it using the forward-invariant set constructed in that paper. However, the results were basically identical to the results with our analytically computed forward-invariant set so we omit them.

In all the examples we started with $P = I$ and $p_a(x, y) = 0$ (planar) or $p_a(x, y, z) = 0$ (three-dimensional), i.e. the initial metric was I . We used polynomials of various degrees, starting with 0 and going up to 10, depending on the system. In all examples we used the exogenous step-size $t_k = 1/k$ and performed 10,000 iterations with the subgradient method. We report the first iteration, where condition (2.2) is fulfilled, i.e. the Riemannian metric is a contraction metric on the forward-invariant set, and the lowest value for ν in (2.2) that we computed overall, or equivalently the best solution found in (4.3). We also report the time needed for the iterations, but these are mainly for comparing the execution times for polynomials of different degrees.

We adapted the software from [27] to compute the metrics. The maximization (4.5) is performed on a 1000×1000 grid for the planar systems with a subsequent refinement on a grid of equal size around the located maximum. Similarly, for the three-dimensional example we used a grid with $500 \times 50 \times 100$ points with refinement on a grid with equal size for the maximization. The metrics for the planar systems were computed on AMD ThreadRipper 3990X (64 cores) and the three-dimensional system on Intel i9900K (8 cores).

5.1. Example: Time-reversed van der Pol system. Consider the time-reversed van der Pol system

$$\begin{pmatrix} \dot{x} \\ \dot{y} \end{pmatrix} = f(x, y) = \begin{pmatrix} -y \\ x - 3(1 - x^2)y \end{pmatrix}. \quad (5.1)$$

Let K be the quadrilateral with vertices (a, d) , (b, c) , $(-a, -d)$, $(-b, -c)$ with $a = 0.6$, $b = 1$, $c = 0.18$, and $d = 2.5$. It is not difficult to verify analytically that K is forward-invariant for the system, see Appendix A. The Jacobian of f at the origin is $Df(0, 0) = \begin{pmatrix} 0 & -1 \\ 1 & -3 \end{pmatrix}$ and has eigenvalues $\lambda_{\pm} = \frac{-3 \pm \sqrt{5}}{2}$. Hence, the largest eigenvalue is $\lambda_+ = \frac{-3 + \sqrt{5}}{2} \approx -0.381966011250105$ and the origin is locally exponentially stable.

Results after iterating over the forward-invariant set K 10,000 times, using different degrees of polynomials, from $p(x, y) = 0$ to $p(x, y) = \sum_{|\alpha| \leq 10} a_\alpha x^\alpha$, can be seen in Table 1.

Time-reversed van der Pol (5.1)

degree	first neg. itr.	lowest $-\nu$	time
0	∞	1.447348563020335	445 s
1	∞	1.448404890308665	468 s
2	2	-0.3133495012442786	545 s
3	7	-0.2952854122048584	639 s
4	3	-0.3692555275877225	885 s
5	7	-0.357751157505084	1134 s
6	3	-0.3639232968985002	1439 s

TABLE 1. Results for the time-reversed van der Pol system (5.1). The degree of the polynomial in the metric is in the first column and the second column contains the first iteration where $-\nu < 0$, i.e. exponential stability is asserted (∞ when $-\nu \geq 0$ for all iterations). The third column reports the lowest value for $-\nu$ in 10,000 iterations and the last column reports the time needed for the computation of the 10,000 iterations on AMD ThreadRipper 3990X (64 cores).

Using a polynomial of degree 2 or higher results in a negative value for $-\nu$ after a few iterations, proving the existence of a unique equilibrium in the forward-invariant set that is exponentially stable. The lowest value obtained for $-\nu$ in 10,000 iterations was -0.3692555275877225 using the polynomial of degree 4. The value $|-\nu| = \nu$ gives a lower bound on the rate of exponential attraction and should be compared to $|\lambda_+| = \left| \frac{-3+\sqrt{5}}{2} \right| \approx |-0.381966011250105|$. Table 2 gives the details of this matrix-valued function. Figure 1 shows the metric $M(x) = e^{p_a(x)}P$ by plotting ellipses of equal distance with respect to the metric around each point, while Figure 2 displays $p_a(x)$.

Note that SOS was used to compute a contraction metric for a slightly different van-der-Pol example [6]; while in their paper degree 4 polynomials were necessary, we already succeeded in finding a contraction metric with a degree 2 polynomial.

5.2. Example: Speed control system. Consider the ODE

$$\begin{pmatrix} \dot{x} \\ \dot{y} \end{pmatrix} = f(x, y) = \begin{pmatrix} y \\ -K_d y - x - g x^2 \left(\frac{y}{K_d} + x + 1 \right) \end{pmatrix}, \quad (5.2)$$

with $K_d = 1$ and $g = 6$, was used in [11, 9, 25] as a model for a speed-control system. The system has two asymptotically stable equilibria, one at $(0, 0)$ and one at $\left(-\frac{\sqrt{3}}{6} - \frac{1}{2}, 0\right) \approx (-0.7887, 0)$, as well as a saddle point at $\left(\frac{\sqrt{3}}{6} - \frac{1}{2}, 0\right) \approx (-0.2113, 0)$. We will consider both asymptotically stable equilibria; first, we look at the one at $(0, 0)$.

This system was considered in [19] and we use the forward invariant sets numerically computed therein and visually determine a quadrilateral, on which we compute our metric, that is a superset of the forward invariant set. For the equilibrium at $(0, 0)$ see Fig. 3.

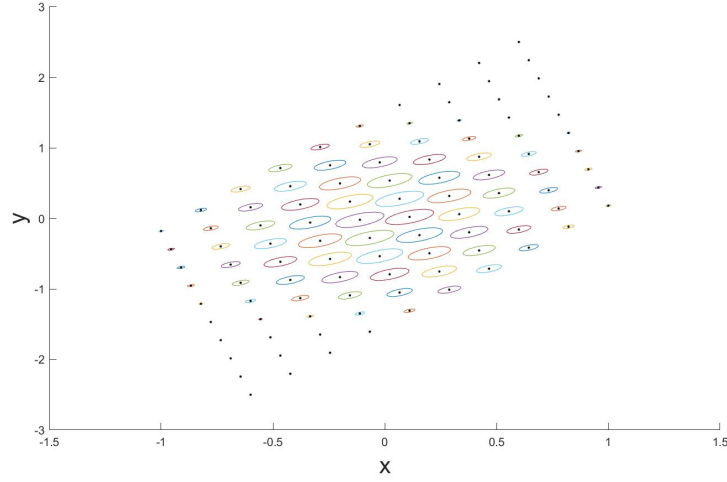


FIGURE 1. Visualization of the optimal metric, see Table 2, obtained for the time-reversed van der Pol system (5.1) on the area K using a 4th degree polynomial and 10,000 iterations. The ellipse around a point $x_0 \in \mathbb{R}^2$ denotes the points of equal distance to the point with respect to the metric, i.e. $\{x \in \mathbb{R}^2 \mid (x - x_0)^\top M(x_0)(x - x_0)^\top = c^2\}$ with fixed $c > 0$.

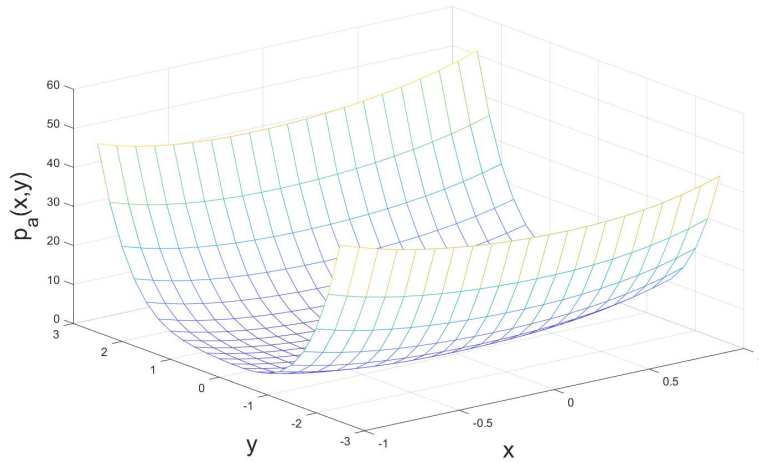


FIGURE 2. Visualization of the polynomial over the area K using a 4th degree polynomial and 10,000 iterations. Since $M(x_0) = e^{p(x_0)}P$, the shape of the ellipse in Figure 1 is the same in the entire area due to P , and we hence show $p_a(x, y)$ in this figure.

Metric $M(x, y) = e^{p_a(x, y)} P$ with $\deg(p_a) = 4$ computed for the time-reversed van der Pol system (5.1) on K with $\nu = 0.3692555275877225$.

$$P = \begin{pmatrix} 1.234732514104349 & -0.7185909507149911 \\ -0.718590950714991 & 1.228098342871417 \end{pmatrix}$$

$p_a(x, y)$			
term	coefficient	term	coefficient
x	0.005874011679514269	xy^2	-0.023594561234174
y	0.002544185767556669	y^3	0.2025391618590853
x^2	3.133966383013717	x^4	1.61103471945693
xy	-0.6857166309584187	x^3y	-0.2487310019195522
y^2	0.3002580326389737	x^2y^2	0.3543359078177429
x^3	-0.01456990449537407	xy^3	0.2471473588049839
x^2y	-0.05483029835239338	y^4	0.9675867347507244

TABLE 2. The contraction metric with the best bound on the exponential rate of attraction for (5.1).

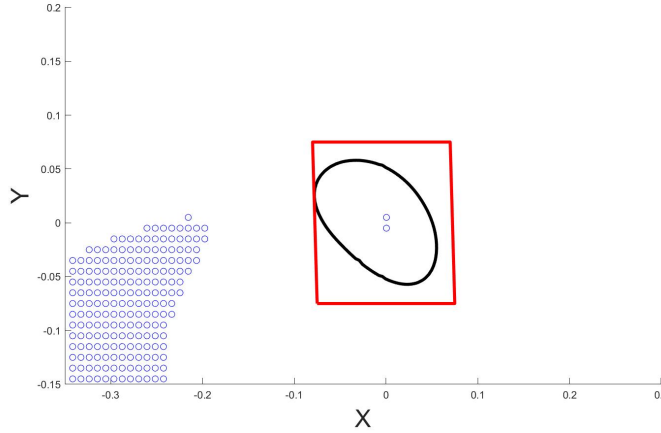


FIGURE 3. The black curve is the forward-invariant set computed in [19] for system (5.2) and the red quadrilateral is the area, on which we compute metrics for the equilibrium at $(0, 0)$. The black curve is a level set of the approximation v of the solution of $V'(x) = -\sqrt{10^{-8} + \|f(x)\|^2}$, while the blue circles denote the areas where $v'(x) \geq 0$. Since the black curve does not touch any blue circles, it is a forward-invariant set.

The Jacobian for f in (5.2) is given by

$$Df(x, y) = \begin{bmatrix} 0 & 1 \\ -1 - 12xy - 18x^2 - 12x & -1 - 6x^2 \end{bmatrix}. \quad (5.3)$$

At the equilibrium $(0, 0)$, we get the eigenvalues $\lambda_{\pm} = \frac{-1 \pm i\sqrt{3}}{2}$, and therefore the lower bound for $-\nu$ is -0.5 .

For the equilibrium $(-0.7887, 0)$, the eigenvalues are $\lambda_1 = -0.6731$ and $\lambda_2 = -4.0590$, so we get the lower bound -0.6731 . In Table 3, the outcome for different degrees of the polynomial is shown. The lowest value for $-\nu$ is obtained with a polynomial of degree 6, but the difference in the outcome is very small between a polynomial of degree 3 and 6.

Speed Control system (5.2) at equilibrium $(0, 0)$

degree	first neg. itr.	lowest $-\nu$	time
0	∞	0.02658980657159118	431 s
1	1628	-0.003808211430038129	462 s
2	1085	-0.004862705555080483	546 s
3	1081	-0.004874280676476273	688 s
4	1081	-0.004874531739145288	860 s
5	1081	-0.004874532732511677	1097 s
6	1081	-0.004874532751723261	1419 s

TABLE 3. Results for the Speed Control system (5.2) at equilibrium $(0, 0)$. The degree of the polynomial in the metric is in the first column and the second column contains the first iteration where $-\nu < 0$, i.e. exponential stability is asserted (∞ when $-\nu \geq 0$ for all iterations). The third column reports the lowest value for $-\nu$ in 10,000 iterations and the last column reports the time needed for the computation of the 10,000 iterations on AMD ThreadRipper 3990X (64 cores).

Figure 4 shows the polynomial $p_a(x, y)$ of degree 6 obtained for the Speed Control system centered around the point $(0, 0)$.

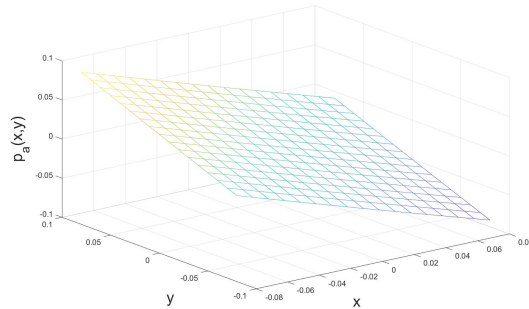


FIGURE 4. Graph of the 6th degree polynomial $p_a(x, y)$ in the metric $M(x, y) = e^{p_a(x, y)} P$ computed with the algorithm for the Speed Control system (5.2) at the equilibrium at $(0, 0)$. Note that it is not a Lyapunov function, in contrast to the construction in the proof of Theorem 3.1.

Metric $M(x, y) = e^{p_a(x, y)}P$ with $\deg(p_a) = 6$ computed for the Speed Control system (5.2) at the equilibrium at $(0, 0)$ on K with $\nu = 0.004874532751723261$.

$$P = \begin{pmatrix} 1.188908218579773 & 0.5845677238765539 \\ 0.5845677238765541 & 1.128530699703952 \end{pmatrix}$$

$p_a(x, y)$			
term	coefficient	term	coefficient
x	-0.6406990025124931	x^5	-0.0001312413688617601
y	0.5224323624975147	x^4y	0.000103857484910813
x^2	0.1189296701550616	x^3y^2	$-8.838844320265229 \cdot 10^{-5}$
xy	-0.07400507177495169	x^2y^3	$8.619846913687634 \cdot 10^{-5}$
y^2	0.06034845248479573	xy^4	$-5.08894875827791 \cdot 10^{-5}$
x^3	-0.01228598722340182	y^5	$7.926099979155098 \cdot 10^{-5}$
x^2y	0.009450037931185229	x^6	$1.458034136517088 \cdot 10^{-5}$
xy^2	-0.006313699379560556	x^5y	$-1.311184472170316 \cdot 10^{-5}$
y^3	0.008513732143946087	x^4y^2	$1.072007441348303 \cdot 10^{-5}$
x^4	0.001521991939021997	x^3y^3	$-8.196794919518857 \cdot 10^{-6}$
x^3y	-0.001284245468051136	x^2y^4	$7.786137296316773 \cdot 10^{-6}$
x^2y^2	0.001027217693957349	xy^5	$-3.724746494883292 \cdot 10^{-6}$
xy^3	-0.000539000261930083	y^6	$5.699738404557221 \cdot 10^{-6}$
y^4	0.0006766508585524121		

TABLE 4. The contraction metric with the best bound on the exponential rate of attraction for (5.2).

Now, we look at the equilibrium at $(-0.7887, 0)$. We use the forward invariant set computed in [19] to determine a quadrilateral on which we compute the metrics; this is shown in Fig. 5.

The optimal metric computed for system (5.2) at equilibrium $(-0.7887, 0)$ was

$$M(x) = e^{p(x, y)}P, \quad \text{with } P = \begin{pmatrix} 2.131845621905937 & 0.8330774850487976 \\ 0.8330774850487975 & 0.7946251260824676 \end{pmatrix}$$

and the 10th degree polynomial $p(x, y)$ plotted in Fig. 6 (we do not list the values of the 65 coefficients due to space constraints).

5.3. Example: Moore–Greitzer jet engine model. We consider the Moore–Greitzer jet engine model [32, §2.4] as studied in [7]. The dynamics are described by the ODE

$$\begin{pmatrix} \dot{x} \\ \dot{y} \end{pmatrix} = f(x, y) = \begin{pmatrix} -y - \frac{3}{2}x^2 - \frac{1}{2}x^3 \\ 3x - y \end{pmatrix}. \quad (5.4)$$

The equilibrium at the origin $(0, 0)$ is globally asymptotically stable and we compute our metric on the area $[-0.5, 0.5]^2$. The Jacobian of f at the origin is $\begin{pmatrix} 0 & -1 \\ 3 & -1 \end{pmatrix}$

and has eigenvalues $-\frac{1}{2} \pm i\frac{\sqrt{11}}{2}$; thus, the lower bound for $-\nu$ is -0.5 for the jet engine system.

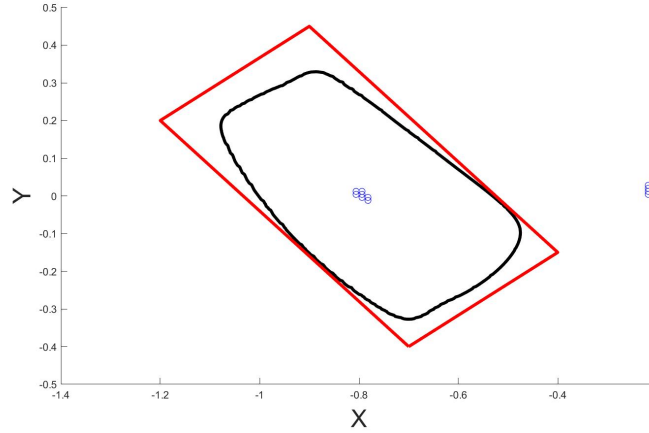


FIGURE 5. The black curve is the forward-invariant set computed in [19] for system (5.2) and the red quadrilateral is the area, on which we compute metrics for the equilibrium at $(-0.7887, 0)$. The black curve is a level set of the approximation v of the solution of $V'(x) = -\sqrt{10^{-8} + \|f(x)\|^2}$, while the blue circles denote the areas where $v'(x) \geq 0$. Since the black curve does not touch any blue circles, it is a forward-invariant set.

Speed Control system (5.2) at equilibrium $(-0.7887, 0)$

degree	first neg. itr.	lowest $-\nu$	time
0	∞	0.1222798935657396	457 s
1	173	-0.05644550658291747	481 s
2	109	-0.01663507890691926	551 s
3	885	-0.01316624664094682	697 s
4	182	-0.04806445535693586	873 s
5	90	-0.1022075700247213	1129 s
6	64	-0.1330993315433471	1413 s
7	54	-0.1486330006840473	1785 s
8	55	-0.1623406730007267	2160 s
9	54	-0.1785195291961935	2607 s
10	56	-0.189294001167907	3092 s

TABLE 5. Results for the Speed Control system (5.2) at equilibrium $(-0.7887, 0)$. The degree of the polynomial in the metric is in the first column and the second column contains the first iteration where $-\nu < 0$, i.e. exponential stability is asserted (∞ when $-\nu \geq 0$ for all iterations). The third column reports the lowest value for $-\nu$ in 10,000 iterations and the last column reports the time needed for the computation of the 10,000 iterations on AMD ThreadRipper 3990X (64 cores).

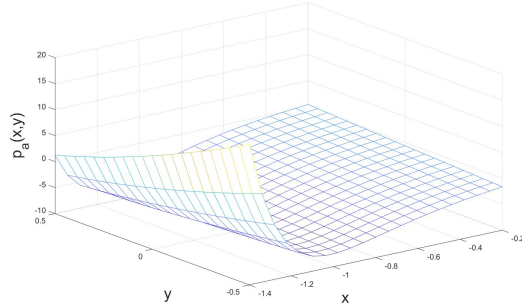


FIGURE 6. Graph of the polynomial $p(x, y)$ in the metric $M(x, y) = e^{p_\alpha(x, y)}P$ for system (5.2) at the equilibrium at $(-0.7887, 0)$, obtained with the algorithm and a polynomial of degree 10.

The SOS method in [7] requires polynomials of degree 4 to find a contraction metric, while we only require degree 2; however, they show global stability. Their lower bound for the rate of exponential convergence $\beta = 2\nu 1.45$ is higher than our rates, however, it is also not compatible with the linear stability analysis above.

We used the method from [19] to compute a forward invariant set from a Lyapunov-like function. The collocation grid was a hexagonal grid on $[-0.6, 0.6]^2$ with density parameter 0.035 and we used the Wendland function $\psi_{5,3}$ with support in $[0, 2]$. The CPA verification was done on a regular triangulation of $[-0.5, 0.5]^2$ with 501×501 vertices. With this method the forward invariant set in the square $[-0.5, 0.5]^2$, depicted in Fig. 7, was computed in less than a second.

The results of our computations are summed up in Table 6.

For a polynomial of degree two and higher the computed metric asserts the exponential stability of the equilibrium. The optimal metric with a 10th degree polynomial computed for system (5.4) at the equilibrium at the origin was

$$M(x) = e^{p(x,y)}P, \quad \text{with} \quad P = \begin{pmatrix} 1.892928154523576 & -0.4408994614637599 \\ -0.44089946146376 & 0.6309760527700889 \end{pmatrix}$$

and the polynomial $p(x, y)$ is plotted in Fig. 8.

5.4. Example: Three dimensional example. Consider the following system:

$$\begin{pmatrix} \dot{x} \\ \dot{y} \\ \dot{z} \end{pmatrix} = f(x, y, z) = \begin{pmatrix} x(x^2 + y^2 - 1) - y(z^2 + 1) \\ y(x^2 + y^2 - 1) + x(z^2 + 1) \\ 10z(z^2 - 1) \end{pmatrix}. \quad (5.5)$$

In Fig. 9, we see the forward invariant set computed in [20] for the system (5.5). The set is contained in the cylinder $C = \{(x, y, z) \in \mathbb{R}^3 \mid |z| \leq 0.6, x^2 + y^2 \leq 0.6^2\}$. We map a cube to C and we compute our metric on it.

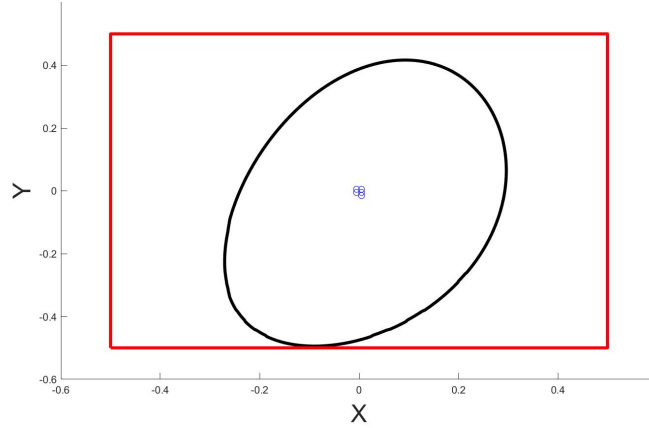


FIGURE 7. The black curve shows the forward-invariant set we computed with the method from [19] for system (5.4) and the red quadrilateral is the area, on which we compute metrics for the equilibrium at the origin. The black curve is a level set of the approximation v of the solution of $V'(x) = -\sqrt{10^{-8} + \|f(x)\|^2}$, while the blue circles denote the areas where $v'(x) \geq 0$. Since the black curve does not touch any blue circles, it is a forward-invariant set.

Moore–Greitzer jet engine model (5.4)

degree	first neg. itr.	lowest $-\nu$	time
0	∞	0.206199297541573	462 s
1	∞	0.2052385876784619	513 s
2	878	-0.01738829435500433	577 s
3	625	-0.01920738923339776	709 s
4	44	-0.06668089661574375	885 s
5	36	-0.06946535756779648	1148 s
6	28	-0.07271224180134611	1426 s
7	28	-0.07323485077040126	1794 s
8	28	-0.07361891063939163	2186 s
9	28	-0.07366357746042262	2621 s
10	28	-0.0737091329581808	3115 s

TABLE 6. Results for the Moore–Greitzer jet engine model (5.4). The degree of the polynomial in the metric is in the first column and the second column contains the first iteration where $-\nu < 0$ and exponential stability is asserted (∞ when $-\nu \geq 0$ for all iterations). The third column reports the lowest value for $-\nu$ in 10,000 iterations and the last column reports the time needed for the computation of the iterations on AMD ThreadRipper 3990X (64 cores).

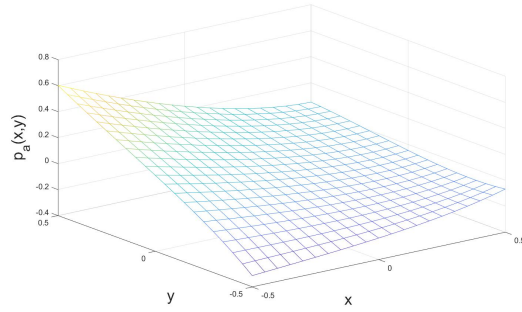


FIGURE 8. Graph of the polynomial $p(x,y)$ in the metric $M(x,y) = e^{p_\alpha(x,y)}P$ for system (5.4) at the equilibrium at the origin, obtained with the algorithm and a polynomial of degree 10.

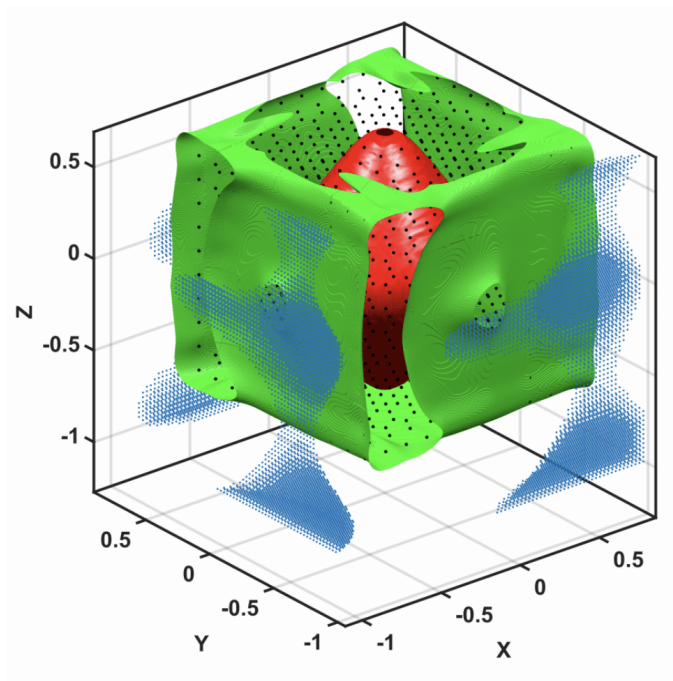


FIGURE 9. The red area in the figure is the forward-invariant set computed in [20] for system (5.5).

Just as in the other examples we can calculate a lower bound for $-\nu$ by calculating the eigenvalues of the Jacobian of the system. The Jacobian of f at the origin has eigenvalues $\lambda_1 = -10$, $\lambda_2 = -1 + i$, and $\lambda_3 = -1 - i$; therefore, the lower bound for $-\nu$ is -1 .

The results of our computations are given in Table 7 and we see that a polynomial of degree 2 or higher delivers a negative values for $-\nu$ in a few iterations. In Table

8 we display the matrix P and the polynomial $p(x, y, z)$ in the optimal metric $M(x, y, z) = e^{p(x, y, z)}P$ computed with $\deg(p) = 2$.

Three dimensional example (5.4)

degree	first neg. itr.	lowest $-\nu$	time
0	∞	0.8099724835857676	7,734 s
1	∞	0.8530578751350688	8,486 s
2	32	-0.1896101138448129	10,889 s
3	48	-0.1712718552180064	17,334 s
4	26	-0.221581678986785	28,712 s
5	30	-0.2160216478649938	45,265 s
6	26	-0.2229981124760225	71,993 s

TABLE 7. Results for the three-dimensional system (5.4). The degree of the polynomial in the metric is in the first column and the second column contains the first iteration where $-\nu < 0$ and exponential stability is asserted (∞ when $-\nu \geq 0$ for all iterations). The third column reports the lowest value for $-\nu$ in 10,000 iterations and the last column reports the time needed for the computation of the iterations on Intel i9900K (8 cores, much slower than the processor used in the other computations).

Optimal metric $M(x, y, z) = e^{p_a(x, y, z)}P$ with $\deg(p_a) = 2$ computed for the system (5.4) at the equilibrium at the origin on the cylinder defined in the text and with $\nu = 0.1896101138448129$.

$$P = \begin{pmatrix} 0.9857018834999954 & -0.000631902183258329 & -5.939756293723396 \cdot 10^{-6} \\ -0.0006319021832583289 & 0.9696657917818603 & -6.827559459905256 \cdot 10^{-6} \\ -5.939756293723396 \cdot 10^{-6} & -6.827559459905256 \cdot 10^{-6} & 1.046242891726449 \end{pmatrix}$$

$p_a(x, y, z)$			
term	coefficient	term	coefficient
x	$2.886921642216002 \cdot 10^{-5}$	xz	-0.01496681273321166
y	$3.103209165308687 \cdot 10^{-6}$	y^2	1.188121045477437
z	$2.350525324502533 \cdot 10^{-7}$	yz	0.02688196544970737
x^2	1.153938280913646	z^2	1.070635223238271
xy	-0.01809571166344076		

TABLE 8. The contraction metric with the best bound on the exponential rate of attraction for (5.4) with a polynomial of degree 2.

In all examples, a contraction metric is found with the proposed algorithm in a few iterations and with a polynomial of low degree. However, the optimal bound is often not realised, even after 10,000 iterations. The bound can, on the other hand, be easily obtained from the Jacobian to the equilibrium.

6. Conclusions. We have proved in Theorem 3.1 that for a system $\dot{x} = f(x)$ with an exponentially stable equilibrium, there necessarily exists a Riemannian contraction metric of the form $M(x) = e^{p(x)}P$. Here p is a polynomial and P a symmetric and positive definite matrix. We adapted the subgradient algorithm for the estimation of the restoration entropy in [28] to compute such metrics and demonstrated the applicability of our new method in four examples.

In comparison to other methods to compute contraction metrics, our method is an iterative and efficient method, which is able to determine compact subsets of the basin of attraction and a lower bound on the rate of exponential attraction.

Appendix A. Forward-invariant set for Example 5.1. We show that quadrilateral with vertices $(a, d), (b, c), (-a, -d), (-b - c)$, $a = 0.6, b = 1, c = 0.18$ and $d = 2.5$, is forward-invariant for system (5.1). First, consider the side from (a, d) to (b, c) . Here, we need to show for $\begin{pmatrix} x \\ y \end{pmatrix} = \begin{pmatrix} b + \theta(a - b) \\ c + \theta(d - c) \end{pmatrix}$ with $\theta \in [0, 1]$ that

$$\begin{pmatrix} -y \\ x - 3(1 - x^2)y \end{pmatrix} \begin{pmatrix} d - c \\ b - a \end{pmatrix} \leq 0.$$

This means

$$\begin{aligned} & -(c + \theta(d - c))(d - c) + \left[b - \theta(b - a) + 3(-1 + b^2 - 2\theta b(b - a) \right. \\ & \quad \left. + \theta^2(b - a)^2)(c + \theta(d - c)) \right] (b - a) \\ &= -c(d - c) + [b - 3(1 - b^2)c](b - a) \\ & \quad + \theta[-(d - c)^2 - (b - a)^2 - 3(1 - b^2)(d - c)(b - a) - 6bc(b - a)^2] \\ & \quad + \theta^2[-6b(b - a)^2(d - c) + 3c(b - a)^3] + \theta^3 3(b - a)^3(d - c) \\ &= -0.0176 - 5.7152\theta - 2.19264\theta^2 + 0.44544\theta^3 =: g_1(\theta) \\ & \leq 0, \end{aligned}$$

since $g_1(0) < 0$ and the derivative of the function is

$$g_1'(\theta) - 5.7152 - 4.38528\theta + 1.33632\theta^2$$

which is strictly negative in $[0, 1]$.

Now, consider the side from $(-a, -d)$ to (b, c) . Here, we need to show for $\begin{pmatrix} x \\ y \end{pmatrix} = \begin{pmatrix} b + \theta(-a - b) \\ c + \theta(-c - d) \end{pmatrix}$ with $\theta \in [0, 1]$ that

$$\begin{pmatrix} -y \\ x - 3(1 - x^2)y \end{pmatrix} \begin{pmatrix} c + d \\ -a - b \end{pmatrix} \leq 0.$$

This means

$$\begin{aligned} & -(c - \theta(c + d))(c + d) + \left[b - \theta(a + b) - 3(1 - (b - \theta(a + b))^2) \right. \\ & \quad \left. (c - \theta(c + d)) \right] (-a - b) \\ &= -c(c + d) + \theta(c + d)^2 \\ & \quad + [b - \theta(a + b) + 3(-1 + b^2 - 2b\theta(a + b) + \theta^2(a + b)^2)(c - \theta(c + d))] (-a - b) \\ &= -c(c + d) + [b + 3(-1 + b^2)c](-a - b) \\ & \quad + \theta[(c + d)^2 + (a + b)^2 + 3(-1 + b^2)(c + d)(a + b) + 6bc(a + b)^2] \end{aligned}$$

$$\begin{aligned}
& + \theta^2[-6b(a+b)^2(c+d) - 3c(a+b)^3] \\
& + \theta^3 3(a+b)^3(c+d) \\
= & -2.0824 + 12.5072\theta - 43.37664\theta^2 + 32.93184\theta^3 =: g_2(\theta) \\
\leq & 0,
\end{aligned}$$

since $g_2(0) = -2.0824 < 0$ and $g_2(1) = -0.02$ and the function has a local maximum in the interval $(0, 1)$ at $\theta_* = 0.181815111989679$ with value

$$g_2(\theta_*) = -1.044364718017452 < 0$$

At the other two sides, the flow is also pointing inward due to symmetry.

REFERENCES

- [1] N. Aghannan and P. Rouchon, [An intrinsic observer for a class of Lagrangian systems](#), *IEEE Trans. Automat. Control*, **48** (2003), 936-944.
- [2] W. Alt, *Numerische Verfahren der Konvexen, Nichtglatten Optimierung*, Teubner, 2004.
- [3] P. N. Anh and L. T. H. An, [New subgradient extragradient methods for solving monotone bilevel equilibrium problems](#), *Optimization*, **68** (2019), 2097-2122.
- [4] P. N. Anh and Q. H. Ansari, [Auxiliary principle technique for hierarchical equilibrium problems](#), *J. Optimiz. Theory App.*, **188** (2021), 882-912.
- [5] P. N. Anh, Q. H. Ansari and H. P. Tu, [DC auxiliary principle methods for solving lexicographic equilibrium problems](#), *J. Global. Optim.*, 2022.
- [6] E. Aylward, P. Parrilo and J.-J. Slotine, Stability and robustness analysis of nonlinear systems via contraction metrics and SOS programming, *LIDS Technical Report 2691*, [arxiv:math/0603313v1](#) (2008), 1-25.
- [7] E. M. Aylward, P. A. Parrilo and J.-J. Slotine, [Stability and robustness analysis of nonlinear systems via contraction metrics and SOS programming](#), *Automatica*, **44** (2008), 2163-2170.
- [8] J. Björnsson and S. Hafstein, Efficient Lyapunov function computation for systems with multiple exponentially stable equilibria, *Procedia Computer Science*, **108** (2017), 655-664, Proceedings of the International Conference on Computational Science (ICCS), Zurich, Switzerland, 2017.
- [9] H.-D. Chiang, M. W. Hirsch and F. F. Wu, [Stability regions of nonlinear autonomous dynamical systems](#), *IEEE Trans. Automat. Control*, **33** (1988), 16-27.
- [10] M. Dellnitz and O. Junge, [Set oriented numerical methods for dynamical systems](#), in *Handbook of Dynamical Systems*, Vol. 2, North-Holland, Amsterdam, 2002, 221-264.
- [11] F. Fallside and M. R. Patel, [Step-response behaviour of a speed-control system with a back-e.m.f. nonlinearity](#), *Proceedings of the Institution of Electrical Engineers*, **112** (1965), 1979-1984.
- [12] O. P. Ferreira, M. S. Louzeiro and L. F. Prudente, [Iteration-complexity of the subgradient method on Riemannian manifolds with lower bounded curvature](#), *Optimization*, **68** (2019), 713-729.
- [13] O. P. Ferreira and P. R. Oliveira, [Subgradient algorithm on Riemannian manifolds](#), *J. Optim. Theory Appl.*, **97** (1998), 93-104.
- [14] P. Giesl, *Construction of Global Lyapunov Functions Using Radial Basis Functions*, Lecture Notes in Math. 1904, Springer, 2007.
- [15] P. Giesl, [Converse theorems on contraction metrics for an equilibrium](#), *J. Math. Anal. Appl.*, **424** (2015), 1380-1403.
- [16] P. Giesl and S. Hafstein, [Construction of a CPA contraction metric for periodic orbits using semidefinite optimization](#), *Nonlinear Anal.*, **86** (2013), 114-134.
- [17] P. Giesl and S. Hafstein, [Review of computational methods for Lyapunov functions](#), *Discrete Contin. Dyn. Syst. Ser. B*, **20** (2015), 2291-2331.
- [18] P. Giesl, S. Hafstein and C. Kawan, [Review on contraction analysis and computation of contraction metrics](#), Accepted at *J. Comp. Dyn.*, **10** (2023), 1-47.
- [19] P. Giesl, S. Hafstein and I. Mehrabinezhad, [Computation and verification of contraction metrics for exponentially stable equilibria](#), *J. Comput. Appl. Math.*, **390** (2021), Paper No. 113332, 21 pp.

- [20] P. Giesl, S. Hafstein and I. Mehrabinezhad, [Computing contraction metrics for three-dimensional systems](#), *IFAC PapersOnLine*, **54** (2021), 297-303.
- [21] P. Giesl and H. Wendland, [Construction of a contraction metric by meshless collocation](#), *Discrete Cont. Dyn. Syst. Ser. B*, **24** (2019), 3843-3863.
- [22] S. F. Hafstein, [A constructive converse Lyapunov theorem on exponential stability](#), *Discrete Contin. Dyn. Syst.*, **10** (2004), 657-678.
- [23] W. Hahn, *Stability of Motion*, Springer, Berlin, 1967.
- [24] C. S. Hsu, [Global analysis by cell mapping](#), *Internat. J. Bifur. Chaos Appl. Sci. Engrg.*, **2** (1992), 727-771.
- [25] L. Jocić, [Planar regions of attraction](#), *IEEE Trans. Automat. Control*, **27** (1982), 708-710.
- [26] T. A. Johansen, [Computation of Lyapunov functions for smooth, nonlinear systems using convex optimization](#), *Automatica*, **36** (2000), 1617-1626.
- [27] C. Kawan, S. F. Hafstein and P. Giesl, [ResEntSG: Restoration entropy estimation for dynamical systems via Riemannian metric optimization](#), *SoftwareX*, **15** (2021), 100743.
- [28] C. Kawan, S. Hafstein and P. Giesl, [A subgradient algorithm for data-rate optimization in the remote state estimation problem](#), *SIAM J. Appl. Dyn. Syst.*, **20** (2021), 2142-2173.
- [29] H. Khalil, *Nonlinear Systems*, 3rd edition, Pearson, 2002.
- [30] N. Krasovskii, *Problems of the Theory of Motion*, Mir, Moscow, 1959. English translation by Stanford University Press, 1963.
- [31] B. Krauskopf and H. M. Osinga, [Computing Invariant Manifolds via the Continuation of Orbit Segments](#), 117-154, Springer Netherlands, Dordrecht, 2007.
- [32] M. Krstic, I. Kanellakopoulos and P. Kokotovic, *Nonlinear and Adaptive Control Design*, Wiley, 1995.
- [33] W. Lohmiller and J.-J. E. Slotine, [On contraction analysis for non-linear systems](#), *Automatica*, **34** (1998), 683-696.
- [34] A. M. Lyapunov, [The general problem of the stability of motion](#), *Internat. J. Control*, **55** (1992), 521-790. Translated by A. T. Fuller from Édouard Davaux's French translation (1907) of the 1892 Russian original. With an editorial (historical introduction) by Fuller, a biography of Lyapunov by V. I. Smirnov, and the bibliography of Lyapunov's works collected by J. F. Barrett, Lyapunov centenary issue.
- [35] G. Osipenko, *Dynamical Systems, Graphs, and Algorithms*, Lecture Notes in Math. 1889, Springer, 2007.
- [36] P. Parrilo, *Structured Semidefinite Programs and Semialgebraic Geometry Methods in Robustness and Optimization*, PhD thesis: California Institute of Technology Pasadena, California, 2000.
- [37] M. M. Peet, [Exponentially stable nonlinear systems have polynomial Lyapunov functions on bounded regions](#), *IEEE Trans. Automat. Control*, **54** (2009), 979-987.
- [38] M. M. Peet and A. Papachristodoulou, [A converse sum of squares Lyapunov result with a degree bound](#), *IEEE Trans. Automat. Control*, **57** (2012), 2281-2293.
- [39] C. Udriste, *Convex Functions and Optimization Methods on Riemannian Manifolds*, vol. 297, Springer Science & Business Media, 2013.
- [40] M. Vidyasagar, *Nonlinear System Analysis*, 2nd edition, Classics in applied mathematics, SIAM, 2002.
- [41] W. Walter, *Ordinary Differential Equation*, Springer, 1998.
- [42] X. Wang, [Subgradient algorithms on Riemannian manifolds of lower bounded curvatures](#), *Optimization*, **67** (2018), 179-194.
- [43] H. Zhang and S. Sra, [First-order methods for geodesically convex optimization](#), *JMLR: Workshop and Conference Proceedings*, **49** (2016), 1-21, <https://arxiv.org/abs/1602.06053>.
- [44] V. Zubov, *Methods of A. M. Lyapunov and their Application*, Translation prepared under the auspices of the United States Atomic Energy Commission; edited by Leo F. Boron, P. Noordhoff Ltd, Groningen, 1964.

Received March 2022; revised November 2022; early access January 2023.